

# Concentration Dependence of Optical Transmission and Extinction of Different Diatom Cultures

Julijana Cvjetinovic<sup>1\*</sup>, Sergei A. Perkov<sup>1</sup>, Maxim A. Kurochkin<sup>1</sup>, Igor S. Sergeev<sup>1,2</sup>,  
Sergey V. German<sup>1</sup>, Yekaterina D. Bedoshvili<sup>3,1</sup>, Nickolai A. Davidovich<sup>4,1</sup>,  
Alexander M. Korsunsky<sup>5</sup>, and Dmitry A. Gorin<sup>1</sup>

<sup>1</sup> Center for Photonic Science and Engineering, Skolkovo Institute of Science and Technology, 30 Bolshoy Boulevard, bld. 1, Moscow 121205, Russia

<sup>2</sup> Laboratory of Laser Biomedicine, FSRC "Crystallography and Photonics" RAS, 59 Leninskiy Prospekt, Moscow 119333, Russia

<sup>3</sup> Limnological Institute, Siberian Branch, Russian Academy of Sciences, 3 Ulan-Batorskaya str., Irkutsk 664033, Russia

<sup>4</sup> T. I. Vyazemsky Karadag Scientific Station, Natural Reserve of the Russian Academy of Sciences, Kurortnoe, Feodosiya 98188, Russia

<sup>5</sup> Department of Engineering Science, University of Oxford, Oxford, OX1 3PJ, United Kingdom

\*e-mail: [julijana.cvjetinovic@skoltech.ru](mailto:julijana.cvjetinovic@skoltech.ru)

**Abstract.** Diatoms are unicellular microalgae enclosed in a hierarchically structured silica cell wall that play a significant role in maintaining the health of the planet's ecosystem. As one of the main photosynthesizers, they are responsible for 20–25% of the world's oxygen release and carbon fixation. In order to develop technologies for the efficient extraction of carbon dioxide, for example, using bioreactors that provide optimal conditions for the growth of diatoms, it is also necessary to effectively track the diatom lifecycle, as well as control parameters that affect their growth. Here we offer a simple device consisting of LED illumination with a central wavelength of 505 nm that allows to monitor changes in diatom concentrations. We examined marine centric and freshwater pennate diatom strains with different morphologies, sizes, and volumes and obtained a linear dependence of the measured transmission on the concentration. The results were compared with the spectrophotometric approach, which showed a higher inaccuracy with respect to the linear fit. We believe that such an optical setup can be used to solve the problems of continuous flow monitoring of algae both in bioreactors as well as in their natural environment. © 2023 Journal of Biomedical Photonics & Engineering.

**Keywords:** diatom algae; optical setup; spectrophotometry; fluorescence; microscopy.

Paper #3567 received 02 Dec 2022; revised manuscript received 06 Dec 2022; accepted for publication 07 Dec 2022; published online 30 Jan 2023. doi: [10.18287/JBPE23.09.010303](https://doi.org/10.18287/JBPE23.09.010303).

## 1 Introduction

Diatoms are the most numerous representatives of phytoplankton, having appeared nearly 200 million years ago [1]. These exquisite single-celled microalgae thrive wherever there is light, water, essential gases and nutrients and play an immense role in keeping the planet's ecosystem working. As one of the main photosynthesizers, they produce about 20–25% of the atmospheric oxygen and form up to a quarter of the organic material [2]. Their most important feature is a highly porous silica cell wall

called frustule, whose intricate patterns and sophisticated designs have captured the attention of researchers for centuries [3, 4]. The silica frustule consists of two halves (valves): the epitheca (the upper part), and the hypotheca (the lower part), joined together by siliceous girdle bands. Diatoms (phylum Bacillariophyta) consists of three classes Coscinodiscophyceae (centric species with radial valve symmetry), Mediophyceae (centric species with radial and bipolar valve symmetry), and the bilaterally symmetric class Bacillariophyceae [5]. Diatoms are extremely diverse, with conservative estimates ranging from 100,000

to 200,000 species, making them one of the most species-rich eukaryotic lineages [6]. Their size ranges from 2 to 1500  $\mu\text{m}$ , although there are a few larger species. In terms of the number of species, pennate diatoms dominate over the centric ones [7]. On the other hand, centric diatoms, which are mainly planktonic, create the bulk of primary production.

Despite their crucial role in the ecosystem, the use of diatoms has previously been almost exclusively limited to academic research. However, owing to their unique structure, abundance, and properties such as high porosity, large surface area, ease of modification, thermal stability, good optical and mechanical properties, efforts have been made to start exploring them for commercial and industrial applications. Over the past 30 years, the potential of diatom frustules as a novel functional material for biomanufacturing and use as gas sensors, drug delivery systems, biosensors, solar cells, SERS platforms, battery electrodes have been examined [8–12]. Moreover, they are indicators of water quality and a source of bioactive substances, such as lipids, omega-3 fatty acids, and proteins [13, 14]. Nowadays, there is a considerable need for optimization of algae bioreactors, both in terms of production efficiency of target algae cultures, and in terms of efficient monitoring of the algal life cycle for cultivation protocols optimization. The growth of diatoms is traditionally assessed by obtaining growth curves upon counting cells under a microscope in selected aliquots. However, many species are prone to aggregation and clustering, therefore, after several days of cultivation, their counting becomes very difficult, especially in the case of small benthic cultures. Probably, the main difficulty in counting cells in a microvolume in a well plate is the impossibility of selecting adequate aliquots, so growth curves are usually presented with rather large technical errors. Diatom cultivation in large bioreactors and subsequent selection of probes would lead to even greater errors.

In order to facilitate the collection and extraction of various bioactive compounds from diatoms, they must not only be grown correctly under optimal conditions, but also effectively monitored. The optical probe methods can selectively analyze the state of diatom cells and monitor their life cycle based on the absorbance and fluorescence of the main light-harvesting pigments: chlorophyll a, chlorophyll c and carotenoids [15]. Chlorophyll a absorbs energy in the violet-blue and orange-red regions of the spectrum, while chlorophyll c mainly absorbs blue and red light [16]. Fucoxanthin, the main carotenoid in diatoms, absorbs in the blue-green part of the spectrum (500–530 nm). Diatoms can be easily studied and visualized with a variety of optical methods, ranging from the historically first light microscopy to modern methods such as fluorescence lifetime imaging and optoacoustic microscopy, which allow studying not only individual cells of diatoms, but also colonies [17]. Moreover, the photoacoustic method in combination with in situ fluorescence imaging has been used to monitor the growth of diatoms during long-term cultivation in the laboratory conditions based on the absorption and fluorescence

signals of the pigments [18–21]. These methods are also promising for studying the activity of these microorganisms in the natural environment, as well as for monitoring their growth in bioreactors or aquaculture installations. Among the current solutions for the bioreactors, some do not allow precise control of growth conditions, as well as continuous monitoring without manual probing [22] and others are designed only for chlorophyll content monitoring [23], whereas the cultivation of diatoms requires monitoring of additional parameters, such as carotenoid content. Moreover, Voznesenskiy et al. showed that temperature dependence of fluorescence intensity of chlorophyll a reflects the specific processes in cells of different microalgae species [24].

In this work, an optical setup consisting of LED illumination with a central wavelength of 505 nm was developed to monitor changes in diatom concentrations. Here, we have selected marine centric and freshwater pennate diatom cultures with different morphologies and sizes to prove the versatility of our method and compared it with results obtained using a commercially available spectrophotometer. We believe that this setup can be used in the future as a component in bioreactors as well as open water bodies for the purpose of continuous flow monitoring of algae.

## 2 Materials and Methods

### 2.1 Diatom Cell Cultures

Here we studied seven different freshwater pennate and marine centric diatom cultures. Pennate diatom cultures (*Asterionella formosa* – strain BZ 33, *Amphipleura* sp. – strain Ov 466, *Hannaea baicalensis* – strain BK 479, *Ulnaria acus* – strain 15k 595) were isolated from a natural population in Lake Baikal and cultivated in the DM medium [25] at 10 °C under natural light and day–night cycle. Marine centric diatoms *Biddulphiopsis titiana* (strain 0.0212-OH, Atlantic ocean), *Coscinodiscus oculus-iridis* (strain 0.1211-OD, Tsushima Strait), *Coscinodiscus* sp. (strain 21.0407-OA, Black sea) were cultivated in ESAW medium prepared according to a modified recipe as described by Polyakova et al. [26] with salinity of ca. 36‰ (0.0212-OH, 0.1211-OD) and 20‰ (21.0407-OA). Cell culture flasks “T-25” (Eppendorf, Germany) with diatom cultures were kept on a windowsill of the laboratory at room temperature under natural light. Sample probes were taken for measurements during the stationary phase of growth.

### 2.2 Visualization of Diatom Algae

Diatoms were visualized and counted under the inverted luminescent microscope NIB-FL (LOMO-MA, Russia) using PH10x and PH40 $\times$  objectives. Images were taken with an UltraHD-4k (35k/s) camera. To determine the concentration of cultures, the flasks with diatoms were thoroughly shaken and 10  $\mu\text{l}$  of each culture was applied to a glass slide in triplicate. For fluorescent visualization, 100  $\mu\text{l}$  of each diatom strain was placed in the individual

well of 96-well plate (CellCarrier Ultra, PerkinElmer, USA) and imaged with a  $\times 20$  and  $\times 60$  magnification objectives using the Operetta High Content Imaging System (Perkin Elmer, USA) in the fluorescence mode. The chlorophyll autofluorescence was excited at 410–430 nm, while the emission was registered at 650–700 nm. The obtained images were processed using Harmony 4.1 software (Perkin Elmer, USA).

### 2.3 Experimental Setup for Optical Monitoring

An optical setup developed to monitor changes in algae concentrations is shown in Fig. 1(a–c). A light emitting diode (LED) with a central wavelength of 505 nm was used as a light source. This wavelength was chosen to match the absorption maximum of carotenoids [27] presented in diatoms, such as fucoxanthin and beta-carotene [16]. The emission spectrum of LED is shown in Fig. 1(d). Emitted light was coupled in a multimode optical fiber with 105  $\mu\text{m}$  core for spatial filtering then collimated by  $f = 7.5$  mm aspheric lens, passed through plastic cuvette with analyzed volume of algae suspended in nutrient medium and measured by a linear photodiode (PD) with preamplifier (OPT101P, Texas Instruments,

USA). The data transfer between the optical system and the personal computer was performed using a microcontroller Arduino Nano. The LED and the photodiode were powered by a 5 V voltage source. The diameter of the probe light beam was 1.5 mm. The PD square shaped photosensitive area size was  $1.7 \times 1.7$  mm. Discretization frequency for Arduino analog-to-digital converter (ADC) was set to 100 Hz. A python code was used to read the data from Arduino, and calculate mean value and standard deviation over 12000 measurements during 2 min. To avoid external illumination influence, the optical setup was covered with a non-transparent enclosure.

LED illumination was coupled into an optical fiber by placing the end of the optical fiber to the LED light-emitting crystal at a distance of 200  $\mu\text{m}$ . For this purpose, a 350  $\mu\text{m}$  diameter hole was drilled in the LED transparent body under the optical control of a stereomicroscope ADF S645. An optical fiber was placed in the LED drilled hole and fixed using epoxy resin as shown on Fig. 1(b). The resulting output power of the LED light output of the collimating aspheric lens was 8.5  $\mu\text{W}$ . Mounting elements of the optical system were produced by photopolymer printing approach.

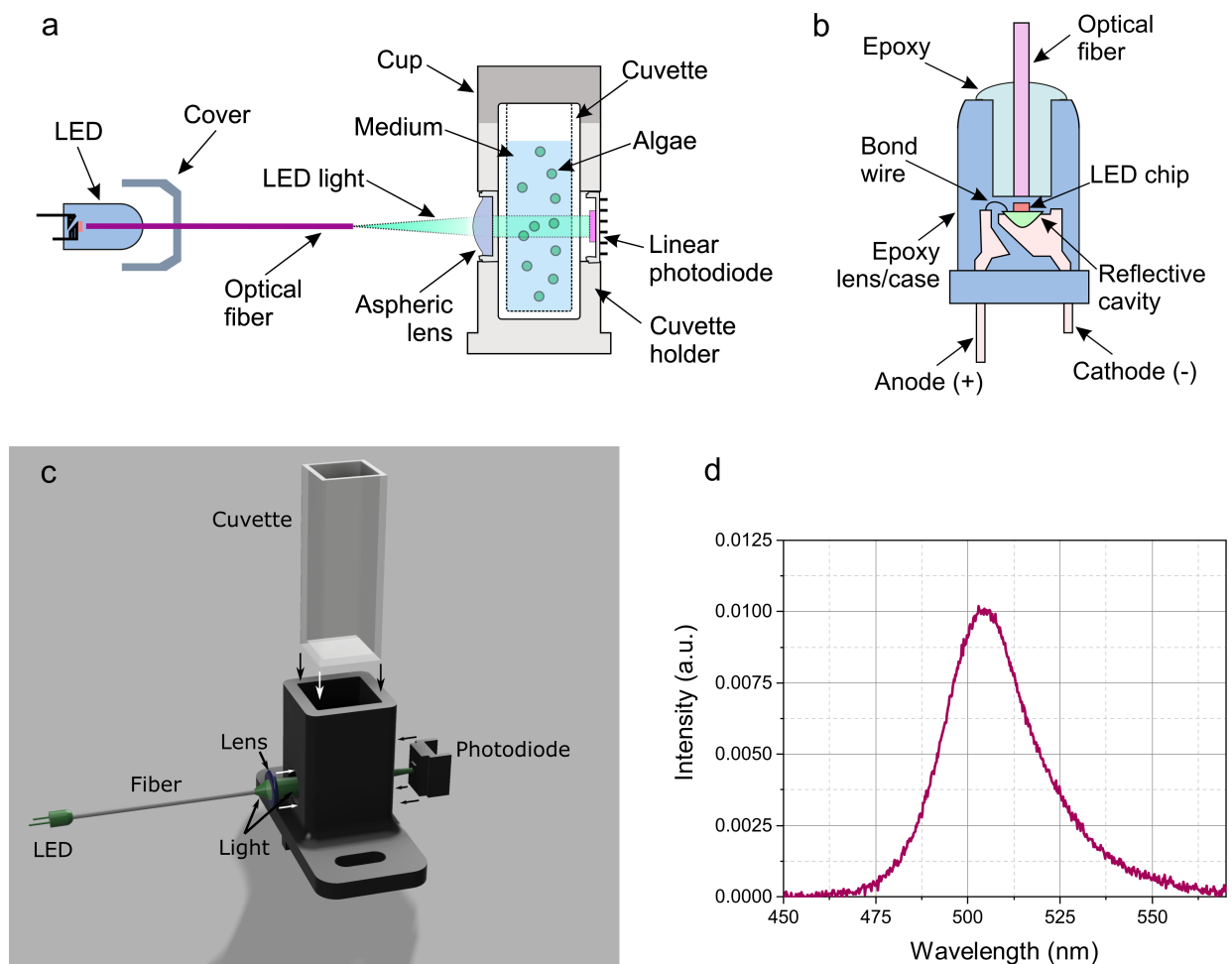


Fig. 1 Experimental setup for monitoring changes in the diatom algae concentration. (a) Artistic representation of an optical system for measuring the transmission of algae in a nutrient medium depending on their fractional dilution. (b) Direct LED light coupling in multimode optical fiber. (c) Schematic representation of the experimental setup key components for transmission measurements. (d) Emission spectrum of LED.

Table 1 Size and morphology of the studied diatom cultures.

No.	Diatom culture (strain number)	Type	Shape	Diameter, $\mu\text{m}$	Length (height), $\mu\text{m}$	Volume, $\mu\text{m}^3$
1	<i>Biddulphiopsis titiana</i> (0.0212-OH)	marine centric	rectangular with round corners	132	255	$3.5 \cdot 10^6$
2	<i>Coscinodiscus oculus-iridis</i> (0.1211-OD)	marine centric	disc-shaped	31	10	$7.5 \cdot 10^3$
3	<i>Coscinodiscus</i> sp. (21.0407-OA)	marine centric	cylindrical	27	36	$2.1 \cdot 10^4$
4	<i>Amphipleura</i> sp. (Ov 466)	freshwater pennate	elliptical	7	57	$2.2 \cdot 10^3$
5	<i>Hannaea baicalensis</i> (BK 479)	freshwater pennate	banana-shaped	7	65	$2.5 \cdot 10^3$
6	<i>Asterionella formosa</i> (BZ 33)	freshwater pennate	single: elongated, star-shaped colonies	5	85	$1.7 \cdot 10^3$
7	<i>Ulnaria acus</i> (15k 595)	freshwater pennate	needle-shaped	5	175	$3.4 \cdot 10^3$

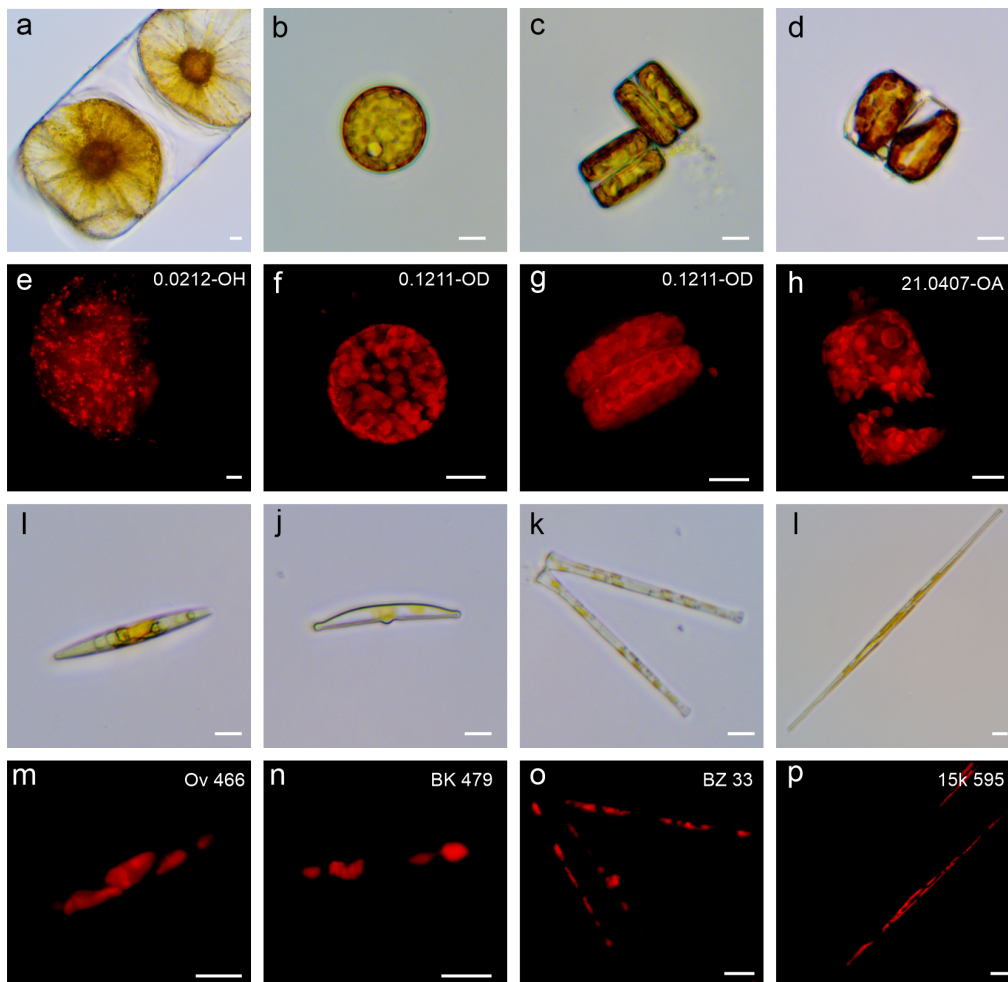


Fig. 2 Brightfield microscopy images of marine centric diatoms: (a) *Biddulphiopsis titiana* (0.0212-OH), *Coscinodiscus oculus-iridis* (0.1211-OD): (b) top view, (c) side view, (d) *Coscinodiscus* sp. (21.0407-OA). Fluorescence images of marine centric diatoms: (e) *Biddulphiopsis titiana* (0.0212-OH), *Coscinodiscus oculus-iridis* (0.1211-OD): (f) top view, (g) side view, (h) *Coscinodiscus* sp. (21.0407-OA). Brightfield microscopy images of freshwater pennate diatoms: (i) *Amphipleura* sp. (Ov 466), (j) *Hannaea baicalensis* (BK 479), (k) *Asterionella formosa* (BZ 33), (l) *Ulnaria acus* (15k 595). Fluorescence images of freshwater pennate diatoms: (m) *Amphipleura* sp. (Ov 466), (n) *Hannaea baicalensis* (BK 479), (o) *Asterionella formosa* (BZ 33), (p) *Ulnaria acus* (15k 595).

## 2.4 Optical Measurements and Spectrophotometry

To verify cell counting ability of the experimental setup, 7 diatom strains were examined. For optical measurements, 1.5 mL of each strain were put into a plastic cuvette in the experimental setup. A custom python script was used to record light intensity values for 2 min, and, subsequently, average them over measurement time and calculate standard deviation. Then, for each strain the sample was diluted  $\times 1.154$  times. This new sample was placed into the experimental setup, and new light intensity values were recorded. This procedure of dilution and measurement was repeated 11 times for each strain. The well-plate with the same 12 dilutions for each of 7 diatoms strains was placed into a spectrophotometer Tecan Infinite M Nano+ (Tecan Trading AG, Männedorf, Switzerland). For all the initial diatoms concentrations extinction and fluorescence spectra (the excitation wavelength was set to 430 nm) were measured. Then for each sample extinction value and fluorescence intensity were measured. Extinction was measured at the wavelength of 505 nm. The fluorescence intensity was registered at 680 nm, when the excitation wavelength was set to 430 nm.

## 3 Results and Discussion

### 3.1 Diatom Algae: Description and Visualization

In this work, we studied 3 marine centric diatom strains and 4 pennate cultures from Lake Baikal with different sizes and morphologies (Table 1, Fig. 2). The diameter and length or height were obtained from brightfield images (Fig. 2), while the volume was calculated for each strain as  $V = \pi (d/2)^2 l$ , where  $d$  is a diameter,  $l$  is a length, approximating diatom cells as cylinders.

Brightfield images of centric (Figs. 2(a–d)) and pennate diatom cells (Figs. 2(i–l)) show how the chloroplast color changes from yellow to golden brown depending on the strain. Fluorescence images demonstrate distribution of chlorophyll throughout the cells (Figs. 2(e–h, m–p)). In the case of *Biddulphiopsis titiana* (0.0212-OH), whose cell size is around 250  $\mu\text{m}$ , chloroplasts partly fill the volume from both sides (Fig. 2(e)). On the other hand, chloroplasts in *Coscinodiscus* species (0.1211-OD, 21.0407-OA) are more densely packed and have oval shape (Figs. 2(f–h)). Figs. 2(c, g) show the side view of *Coscinodiscus oculus-iridis* in the process of division. Chloroplasts in the case of freshwater cultures *Amphipleura* sp. (Ov 466) and *Ulnaria acus* (15k 595) occupy most of the cells (Fig. 2(m, p)), while in *Hannaea baicalensis* (BK 479) and *Asterionella formosa* (BZ 33) they are distributed in the form of grains (Fig. 2(n, o)).

### 3.2 Optical Measurements and Spectrophotometry

The results of measurements obtained using experimental setup described in Fig. 1 are demonstrated in Fig. 3. For each diatom strain measured light intensity values were normalized by the nutrient medium light intensity values, and the concentration values were multiplied by the number of cells in mL, calculated on the microscope for each diatom strain. Standard deviation, that was calculated from 12000 measurements for each sample, cannot be seen on graph because error bars do not exceed the size of a dot. The observed dependence of the measured light intensity on the relative concentration of diatoms was approximated by the linear fit for each diatoms strain. It can be seen that all values have high correlation with the linear fit, and are in a good agreement with Bouguer-Beer-Lambert Law, which states that sample's extinction (light attenuation) has linear dependence on light absorber's concentration:

$$A = \epsilon l C + G_s, \quad (1)$$

where  $A$  is extinction,  $\epsilon$  is molar extinction coefficient,  $l$  is optical path,  $C$  is concentration of chromophores, presented in diatoms,  $G_s$  is the attenuation factor, accounting for scattering and geometry of particles [28].

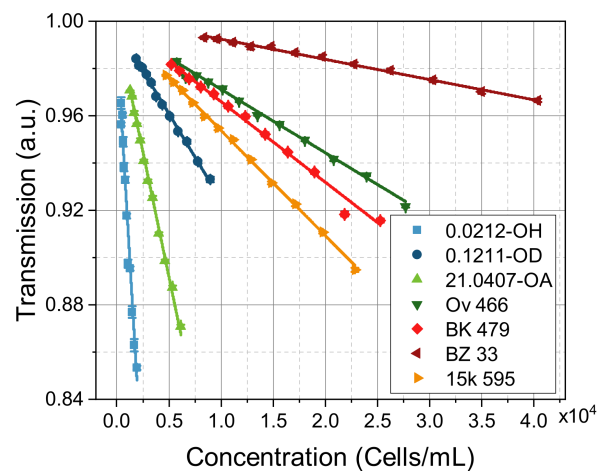


Fig. 3 Optical measurements of diatom cultures. Dependence of light intensity on the relative diatom cell concentrations. Light intensity was normalized on the measurements of nutrient medium. Scatter plot represents measured values, solid lines represent linear fit.

To demonstrate the advantages of our system over conventional spectrophotometric approach and investigate opportunities for future development of the device, the extinction and fluorescence intensity measurements were made. Fig. 4(a) demonstrates extinction spectra for initial concentrations of 7 diatom strains. The dependence of diatoms extinction on the concentration is demonstrated in Fig. 4(b). For all strains measured values were approximated by the linear fit. The

coefficients of determination (COD) for all linear fits are shown in Table 2. It can be seen, that for all strains spectrophotometric measurements demonstrate lower COD values, than optical measurements on the custom setup, which indicates higher accuracy of the latter. This can be explained by the difference in the sensing volume. According to the manufacturer of Tecan Infinite M Nano+, the spot size of the absorbance light beam is 0.7 mm in diameter. The optical path for 200  $\mu$ L sample

is 6.25 mm, thus the sensing volume is  $V = 2.405 \text{ mm}^3$ . In contrast to that, our setup has a spot size of light beam scaled to 1.5 mm in diameter, and the optical path is 10 mm. Therefore, the sensing volume in our setup is  $V = 17.67 \text{ mm}^3$ , which is 7 times greater than in spectrophotometer. This allows our setup to average values more accurately even for small diatom cell concentrations.

Table 2 Comparison of the coefficient of determination (COD) for spectrophotometric measurements with optical measurements on the custom device.

Diatom strain	Spectrophotometer, COD	Custom device, COD
0.0212-OH	0.840	0.981
0.1211-OD	0.954	0.997
21.0407-OA	0.983	0.998
Ov 466	0.929	0.996
BK 479	0.975	0.993
BZ 33	0.638	0.995
15k 595	0.901	0.999

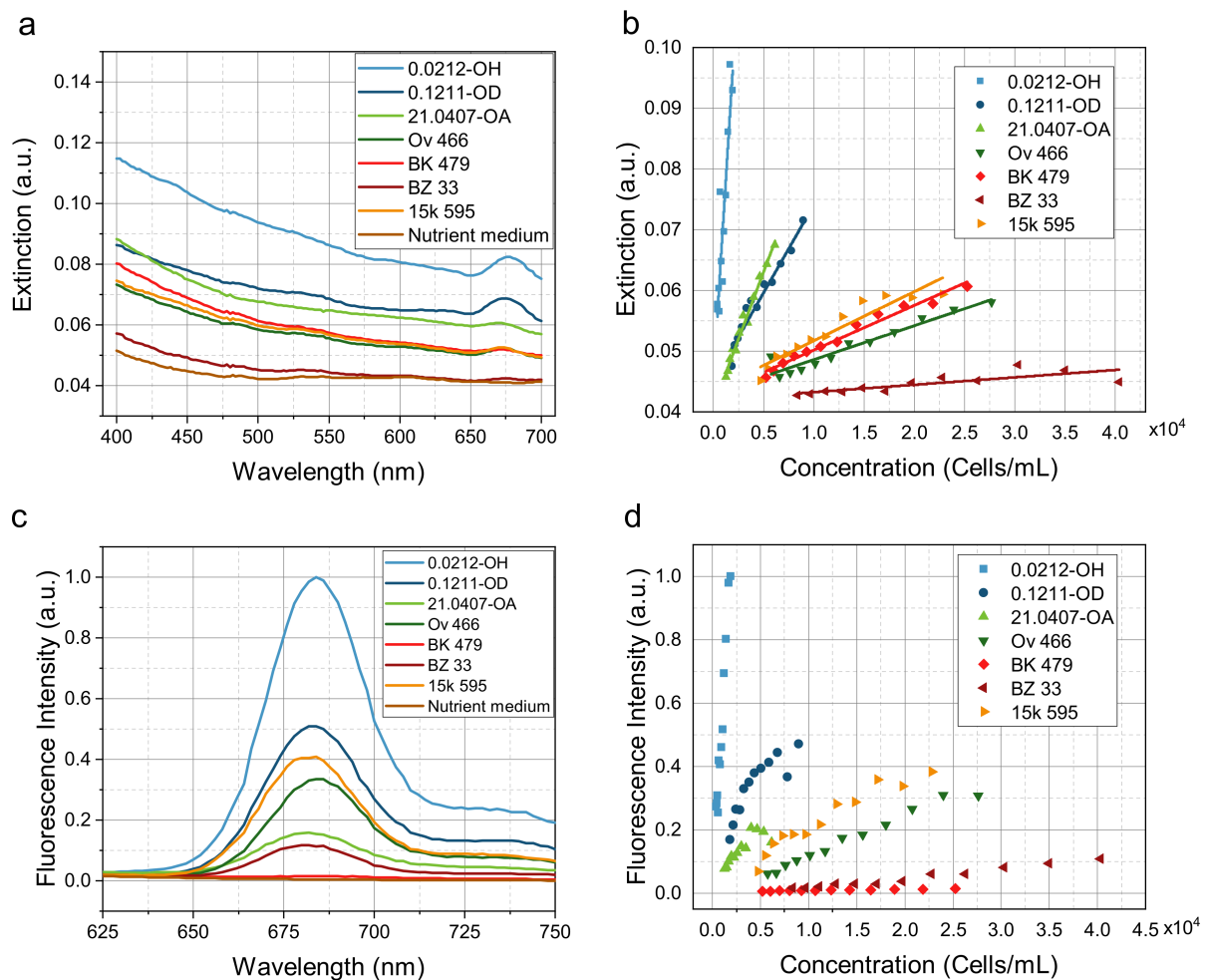


Fig. 4 Spectrophotometric and fluorescence measurements of diatoms. (a) Extinction spectra. (b) Dependence of extinction ( $\lambda = 505 \text{ nm}$ ) on the diatom concentration. Scatter plot represents extinction values normalized on the nutrient medium extinction. Solid lines represent linear fit. (c) Fluorescence intensity spectra. Excitation wavelength: 430 nm. (d) Dependence of fluorescence intensity ( $\lambda_{\text{ex}} = 430 \text{ nm}$ ,  $\lambda_{\text{em}} = 680 \text{ nm}$ ) on the diatom concentration. Scatter plot represents fluorescence intensity values normalized on the nutrient medium values.

Fig. 4(c) demonstrates fluorescence intensity spectra for initial concentrations of 7 diatom strains (excitation wavelength: 430 nm). It can be seen that all strains exhibit fluorescence except for nutrient medium and BK 479 strain. This observation correlates with the absence of extinction peak of chlorophyll *c* in BK 479, that should be located near 680 nm. Brightfield microscopic images and the growth curve allow to assume, that this strain was in the transition between stationary growth phase and the last (death) phase during measurements. The composition and quantity of pigments is not constant and depends on the intensity of light, the spectral composition of light, the content of nutritional elements in water, as well as on the growth phase and the characteristics of diatom vital activity [16, 29]. The amount of chlorophyll somewhat decreases at the end of the stationary phase of growth without renewal of the medium. Thus, fluorescence and extinction measurements of diatoms at the wavelength of 680 nm might be a potential marker of the diatom growth phase.

Also, Fig. 4(d) shows the dependence of fluorescence intensity on the concentration for 7 diatom strains (excitation wavelength: 430 nm, emission wavelength: 680 nm). One can observe, that marine centric diatom cultures (strain No. 0.0212-OH, 0.1211-OD and 21.0407-OA) exhibit stronger fluorescence dependence on concentration than pennate diatom cultures (strain No. 15k 595, Ov 466, BK 479, BZ 33).

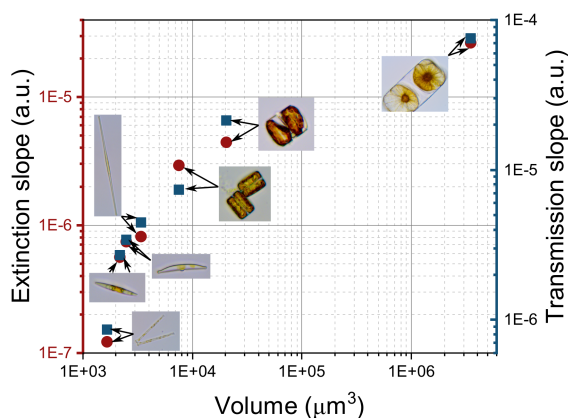


Fig. 5 The dependence of linear fit slopes on the diameter of diatom cells. The red circles represent slopes of linear fit in extinction measurements. The blue squares represent absolute values of slopes of linear fit in transmission measurements on the custom-made setup described in Fig. 1.

It can be noted from Figs. 3 and 4, that slopes of linear fits differ between diatom strains. To be more precise, slope of linear fit is connected to geometrical parameters of a strain, and this dependence is demonstrated in Fig. 5.

One can clearly see the monotonic dependence of the slope on the volume of diatom cells, that was extracted from the Table 1. The relation between slopes of linear fits and diatom volume is similar in both extinction and transmission measurements and mostly determined by the extinction coefficient, that combines absorption and scattering properties of diatoms. This knowledge could be used for more accurate tuning of the photodetector sensitivity for monitoring of each diatom strain and for characterization of diatom biomass.

## 4 Conclusions

In this work capabilities of transmission measurements at the wavelength of 505 nm for 7 diatom strains were demonstrated and compared to the spectrophotometric approach. As a result, the linear dependence of measured transmission on the diatom concentration was observed with high accuracy for all 7 diatom strains. However, for spectrophotometric extinction measurements this dependence exhibits higher inaccuracy when compared to linear fit. Fluorescence measurements suggest that transmission measurements at the wavelength of 680 nm and fluorescence measurements with excitation wavelength of 430 nm and emission wavelength of 680 nm can improve understanding of diatoms life cycles and current state of diatoms in the bioreactor. Also, a monotonic dependence of linear fit slopes for both extinction and transmission measurements on the diatom volume was demonstrated. Thus, it can be concluded that described approach is promising for continuous monitoring of diatoms in bioreactors, and can be improved with addition of transmission measurements at the wavelength of 680 nm and fluorescence measurements with the same emission wavelength, as well as fine tuning of a photodetector sensitivity based on the obtained dependencies of the linear fits on the diatom volume.

## Disclosures

The authors declare that there is no conflict of interest.

## Acknowledgements

The work was supported by Russian Science Foundation (RSF) grant No. 22-14-00209. The investigated marine centric diatom strains were isolated and introduced in a culture thanks to the project number 121032300019-0, Study of Fundamental Physical, Physiological, Biochemical, Reproductive, Population, and Behavioural Characteristics of Marine Hydrobionts funded by the Ministry of Science and Higher Education of the Russian Federation.

## References

1. M. J. Behrenfeld, K. H. Halsey, E. Boss, L. Karp-Boss, A. J. Milligan, and G. Peers, “Thoughts on the evolution and ecological niche of diatoms,” *Ecological Monographs* 91(3), e01457 (2021).
2. S. Malviya, E. Scalco, S. Audic, F. Vincent, A. Veluchamy, J. Poulain, P. Wincker, D. Iudicone, C. de Vargas, L. Bittner, A. Zingone, and C. Bowler, “Insights into global diatom distribution and diversity in the world’s ocean,” *Proceedings of the National Academy of Sciences* 113(11), E1516–E1525 (2016).
3. E. De Tommasi, J. Gielis, and A. Rogato, “Diatom Frustule Morphogenesis and Function: a Multidisciplinary Survey,” *Marine Genomics* 35, 1–18 (2017).
4. A. M. Korsunsky, P. V. Sapozhnikov, J. Everaerts, and A. I. Salimon, “Nature’s neat nanostructuration: The fascinating frustules of diatom algae,” *Materials Today* 22, 159–160 (2019).
5. M. D. Guiry, G. M. Guiry, *AlgaeBase*. World-wide electronic publication, National University of Ireland, Galway (accessed 1 December 2022). [<https://www.algaebase.org>].
6. R. Gordon, D. Losic, M. A. Tiffany, S. S. Nagy, and F. A. S. Sterrenburg, “The Glass Menagerie: diatoms for novel applications in nanotechnology,” *Trends in Biotechnology* 27(2), 116–127 (2009).
7. N. A. Davidovich, O. I. Davidovich, *Reproductive Biology of Diatoms*, ARIAL, LLC, Simferopol (2022). ISBN 978-5-907587-63-2 [in Russian].
8. N. Sharma, D. P. Simon, A. M. Diaz-Garza, E. Fantino, A. Messaabi, F. Meddeb-Mouelhi, H. Germain, and I. Desgagné-Penix, “Diatoms Biotechnology: Various Industrial Applications for a Greener Tomorrow,” *Frontiers in Marine Science* 8, 636613 (2021).
9. A. Bozarth, U.-G. Maier, and S. Zauner, “Diatoms in biotechnology: Modern tools and applications,” *Applied Microbiology and Biotechnology* 82(2), 195–201 (2009).
10. M. Mishra, A. P. Arukha, T. Bashir, D. Yadav, and G. B. K. S. Prasad, “All new faces of diatoms: Potential source of nanomaterials and beyond,” *Frontiers in Microbiology* 8, 1239 (2017).
11. A. M. Korsunsky, Y. D. Bedoshvili, J. Cvjetinovic, P. Aggrey, K. I. Dragnevski, D. A. Gorin, A. I. Salimon, and Y. V. Likhoshway, “Siliceous diatom frustules – A smart nanotechnology platform,” *Materials Today: Proceedings* 33(4), 2032–2040 (2020).
12. P. Aggrey, M. Nartey, Y. Kan, J. Cvjetinovic, A. Andrews, A. I. Salimon, K. I. Dragnevski, and A. M. Korsunsky, “On the diatomite-based nanostructure-preserving material synthesis for energy applications,” *RSC Advances* 11(51), 31884–31922 (2021).
13. H.-Y. Li, Y. Lu, J.-W. Zheng, W.-D. Yang, and J.-S. Liu, “Biochemical and genetic engineering of diatoms for polyunsaturated fatty acid biosynthesis,” *Marine Drugs* 12(1), 153–166 (2014).
14. I. Barkia, L. Al-Haj, A. Abdul Hamid, M. Zakaria, N. Saari, and F. Zadjali, “Indigenous marine diatoms as novel sources of bioactive peptides with antihypertensive and antioxidant properties,” *International Journal of Food Science & Technology* 54(5), 1514–1522 (2019).
15. A. Burson, M. Stomp, E. Greenwell, J. Grosse, and J. Huisman, “Competition for nutrients and light: testing advances in resource competition with a natural phytoplankton community,” *Ecology* 99(5), 1108–1118 (2018).
16. P. Kuczynska, M. Jemiola-Rzeminska, and K. Strzalka, “Photosynthetic pigments in diatoms,” *Marine Drugs* 13(9), 5847–5881 (2015).
17. J. Cvjetinovic, A. I. Salimon, M. V. Novoselova, P. V. Sapozhnikov, E. A. Shirshin, A. M. Yashchenok, O. Yu. Kalinina, A. M. Korsunsky, and D. A. Gorin, “Photoacoustic and fluorescence lifetime imaging of diatoms,” *Photoacoustics* 18, 100171 (2020).
18. J. Cvjetinovic, Y. Bedoshvili, D. Nozdriukhin, O. Efimova, A. Salimon, N. Volokitina, A. Korsunsky, and D. Gorin, “In situ fluorescence / photoacoustic monitoring of diatom algae,” *Proceedings of SPIE* 11641, 116410G (2021).
19. J. Cvjetinovic, A. I. Salimon, M. V. Novoselova, P. V. Sapozhnikov, O. Y. Kalinina, A. M. Korsunsky, and D. A. Gorin, “Photoacoustic visualization of diatom algae,” *Limnology and Freshwater Biology* 3(4), 779–780 (2020).
20. J. Cvjetinovic, Y. D. Bedoshvili, D. V. Nozdriukhin, A. I. Salimon, A. M. Korsunsky, and D. A. Gorin, “Photonic tools for evaluating the growth of diatom colonies during long-term batch cultivation,” *Journal of Physics: Conference Series* 2172(1), 012011 (2022).
21. J. Cvjetinovic, D. V. Nozdriukhin, Y. D. Bedoshvili, A. I. Salimon, A. M. Korsunsky, and D. A. Gorin, “Assessment of diatom growth using fluorescence imaging,” *Journal of Physics: Conference Series* 1984, 012017 (2021).
22. L. Rodolfi, N. Biondi, A. Guccione, N. Bassi, M. D’Ottavio, G. Arganaraz, and M. R. Tredici, “Oil and eicosapentaenoic acid production by the diatom *Phaeodactylum tricorutum* cultivated outdoors in Green Wall Panel (GWP®) reactors,” *Biotechnology and Bioengineering* 114(10), 2204–2210 (2017).
23. T. Yu. Plyusnina, S. S. Khruschev, N. S. Degtereva, I. V. Konyukhov, A. E. Solovchenko, M. Kouzmanova, V. N. Goltsev, G. Yu. Riznichenko, and A. B. Rubin, “Gradual changes in the photosynthetic apparatus triggered by nitrogen depletion during microalgae cultivation in photobioreactor,” *Photosynthetica* 58(Special Issue), 443–451 (2020).

24. S. S. Voznesenskiy, E. L. Gamayunov, A. Yu. Popik, Zh. V. Markina, and T. Yu. Orlova, “[Temperature dependence of the parameters of laser-induced fluorescence and species composition of phytoplankton: The theory and the experiments](#),” *Algal Research* 44, 101719 (2019).
25. A. S. Thompson, J. C. Rhodes, and I. Pettman, *Culture Collection of Algae and Protozoa: Catalogue of Strains*, Amblesibe, UK (1998).
26. S. L. Polyakova, O. I. Davidovich, Y. A. Podunay, and N. A. Davidovich, “[Modification of the ESAW culture medium used for cultivation of marine diatoms](#),” *Marine Biological Journal* 3(2), 73–80 (2018).
27. R. Croce, H. Van Amerongen, “[Natural strategies for photosynthetic light harvesting](#),” *Nature Chemical Biology* 10, 492–501 (2014).
28. V. V. Tuchin (Ed.), *Tissue Optics: Light Scattering Methods and Instruments for Medical Diagnosis*, 3<sup>rd</sup> Ed., SPIE Digital Library, USA (2015). ISBN: 9781628415162.
29. E. S. Holdsworth, “[Effect of growth factors and light quality on the growth, pigmentation and photosynthesis of two diatoms, \*Thalassiosira gravida\* and \*Phaeodactylum tricorutum\*](#),” *Marine Biology* 86, 253–262 (1985).